

WIND-DRIVEN SAND MOTION ACROSS MARS AND IMPLICATIONS FROM ORBITAL ANALYSIS. M. Chojnacki¹, L. Fenton², M. Banks³, S. Silvestro^{2,4}, D. Vaz⁵, A. Urso¹, R.C. Ewing⁶, and M. Lapotre⁷. ¹Lunar and Planetary Lab, University of Arizona, Tucson, AZ (chojan1@pirl.lpl.arizona.edu), ²SETI Institute, Mountain View, CA, ³NASA Goddard Space Flight Center, Greenbelt, MD, ⁴INAF Osservatorio Astronomico di Capodimonte, Napoli, Italy, ⁵Centre for Earth and Space Research of the University of Coimbra, Portugal, ⁶Texas A&M University, College Station, TX, ⁷Harvard University, Cambridge, MA.

Introduction: The last half-decade of Mars exploration has greatly enhanced our knowledge of the active Martian surface. Wind-driven sand motion has been firmly established by the observations of active sand ripples and dunes. Orbital-based studies have shown spatial variations in bedform activity [1–3] and quantified size-independent volumetric sand fluxes [4–9], while surface rovers provide critical details on local conditions [10–14]. The purpose of this abstract is to update the community on major advances in our knowledge of contemporary aeolian bedform dynamics across Mars, including: the range of bedform classes, relevant boundary conditions, spatial and temporal trends, possible transport modes, and implications for landscape evolution. This report also provides an update to several overarching observations, which were put forward at the 8th International Conference on Mars led by the late Nathan Bridges [1].

Datasets and methods: The main dataset utilized to assess aeolian activity at a global scale consists of images acquired by the High Resolution Imaging Science Experiment (HiRISE) camera (0.25–0.5 m/pix). Bedform dynamics can be assessed with simple manual (local) image registration [1, 2], full image orthorectification from stereo-photogrammetry [7, 8], and/or precise tracking of ripple movement using COSI-Corr software [4, 5, 9]. These methods are greatly supplemented by the information gained from *in situ* rover observations [10–14] – see Lapotre *et al.* (*this conference*) for an update.

Overarching results:

(1) *Active sand dune metrics:* Active bedform heights, migration rates, and sand fluxes all span two to three orders of magnitude across Mars. Heights for migrating sand dunes vary widely (2–120 meters tall), but most are 15–25 meters-tall [8]. Global studies show average dune migration rates converge around 0.5 m/yr ($1\sigma \pm 0.4$ m/yr), dune crest fluxes are near 7.8 ± 6.4 (1σ) $\text{m}^3 \text{m}^{-1} \text{yr}^{-1}$, and the highest flux for an individual dune is $35 \text{ m}^3 \text{m}^{-1} \text{yr}^{-1}$ [3, 8]. The Bagnold Dunes of Gale crater, investigated by the *Curiosity* rover, show lower rates (0.2 m/yr) and fluxes ($1 \text{ m}^3 \text{m}^{-1} \text{yr}^{-1}$) [7, 12, 13].

(2) *Sand dune activity and sediment fluxes show regional heterogeneity:* The highest sand fluxes are concentrated in three regions: Syrtis Major, Hellespontus Montes, and the North polar erg [8]. These regions are located near prominent transition zones of topography (e.g., basins, polar caps) and thermophysical properties

(e.g., albedo variations). These boundary conditions, along with the presence of seasonal volatiles, have been proposed to contribute to large-scale slope winds as a driver of sand movement [8]. In contrast, dune-field-scale topography and roughness will cause thickening of the internal boundary layer, resulting in decreased sand transport [9]. Site elevation, and its indirect effects on saltation threshold with pressure, is another global control impacting sand mobility [3].

(3) *North polar erg:* Recognized early as a prominent region for active bedforms [1], north polar dunes display the greatest migration rates and fluxes [8], despite a state of limited sediment availability for half of the martian year due to seasonal autumn/winter $\text{CO}_2/\text{H}_2\text{O}$ ice accumulation. This seasonal CO_2 ice appears to contribute to up to 20% of the local sand movement in the form of large slipface alcoves that develop during the colder seasons and are driven by seasonal frost [15]. Spring and summer katabatic winds are driven by the retreat of the seasonal CO_2 and increasingly large thermal and albedo change (15–25%), while steered zonally by Coriolis-force directed winds [8, 16].

(4) *South polar dune fields:* In vast contrast to the north polar erg, southern dune fields (<45°S) are less active [3]. Southward of 57°S, some slowly migrating ripples are detected [3, 8] but dunes south of this latitude appear static and without crisp slipfaces [3, 17]. These contrasts in morphology and sand mobility are attributed to the greater relief and katabatic winds of the northern cap, along with the longer and colder winters (longer duration of frost) and higher regional elevation (lower surface pressure) in south polar areas [3, 8, 17].

(5) *Abrasion rates and landscape evolution:* Abrasion rates of local basaltic bedrock are estimated to be 0.1–25 $\mu\text{m}/\text{yr}$ for flat ground and 1–120 $\mu\text{m}/\text{yr}$ for a vertical rock face [1, 4, 7]. The abrasion susceptibility of softer sedimentary terrains composed of clays and sulfates will allow for greater erosion [7]. Recognizing these units is important, as sand blasting may rapidly expose potential organic-bearing sedimentary layers, minimizing degradation due to cosmic rays [18] – thus providing favorable conditions for sampling by future missions [7]. Abrasion of sedimentary deposits over deep geologic time can also lead to young exposure ages and contribute to landscape evolution [19].

(6) *Temporal trends in sand transport:* Sand transport will be greater during periods of higher

atmospheric pressure as the threshold friction speed would be depressed [3]. Seasonal monitoring of ripples [5] showed the greatest fluxes during perihelion (estimated local pressure of 6.3 mbar), while they were lowest during aphelion (5.3 mbar). This ~15% change in air pressure resulted in a three-fold increase in sand fluxes [5, 7]. Locations with annual measurements from different years indicate sand fluxes can vary by a factor of five, providing evidence for years of enhanced sand transport [20]. Other sites show bedform fluxes that are nearly identical from year-to-year, indicating a typical annual wind regime for some areas [20, 21]. Winds from planet-encircling dust events (e.g., 2007, 2018) may also enhance or retard sand transport rates [6, 10, 22].

(7) *Dark-toned ripples (DTRs)*: The activity of meter-scale (1-5 m spacing and ~40 cm tall) DTRs [1, 3, 8, 14] is quite variable. Active DTRs are typically associated with dark dunes [23], but may also occur as isolated sand patches (Jezero crater delta), and on steep slopes (20-30°) where Recurring Slope Linea (RSL) form [24]. This contrasts with the inactivity for ripples of a similar scale in Meridiani Planum (near *Opportunity*) [25, 26] and Gusev crater (near *Spirit*) [7, 10] (**Fig. 1**). Some of these DTRs have been constrained to be inactive to ~50-200 ka, thought to be due to their stabilization via a lag of coarse material [25, 26].

(8) *Megaripples and Transverse Aeolian Ridges (TARs)*: Larger ripples (spacing of ~8-18 m and heights of 0.8-2 m), variable in tone, have also been observed to migrate similar to, and in continuity with DTRs (**Fig. 1**) [8, 27]. This may suggest that these decameter-scale megaripples exist on a continuum of Martian bedforms from DTRs to TARs. TARs are light-toned, moderate-scale (10-100 m spacing and 1-14 m tall) bedforms, with a debated origin [28, 29], but have been widely-accepted to have been inactive based on lack of change and super-position relationships [1, 10, 30]. New detections of TAR migration in a few locations might suggest

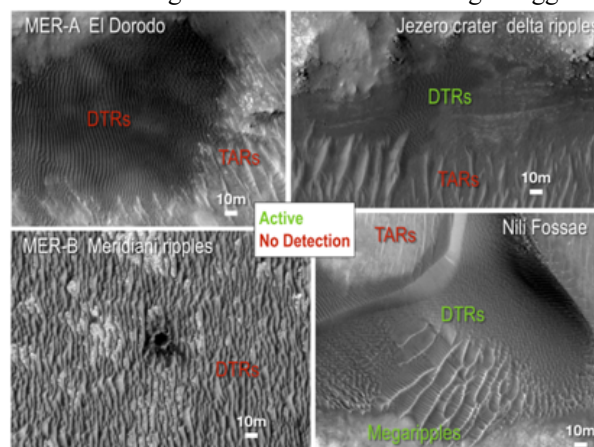


Figure 1. Four bedform sites in HiRISE at that same scale. TARs, DTRs, and megaripples are shown.

some of these bedforms are in a state of low activity, rather than completely stabilized and a relic of past climates [31].

(9) *Modes of transport*: Whereas decimeter-scale impact ripples, common to landing sites and terrestrial deserts, likely form from impact processes (i.e., hopping or saltating/reptating grains) [32], decameter DTRs on Mars have a more debated origin. *Curiosity's* exploration of the Bagnold Dunes has provided new insight into DTRs [12]. It has been suggested that DTRs form analogously to terrestrial current ripples, which may develop from Martian winds because of the planet's higher kinematic viscosity (caused by the low-density atmosphere) [14]. Another proposed mechanism suggests that "saltation clusters", which develop as sand particles are aerodynamically entrained at speeds between the impact and fluid velocity thresholds [11], conspire to form meter-scale ripples [33]. It is unclear if these mechanisms apply to larger scale megaripple bedforms (>10 m wavelengths) found in continuity with DTRs (**Fig. 1**) [27]. Dune transport under high sand availability is frequently recognized as developing under "bed instability mode" [34]. In contrast, conditions of low sediment supply form dunes in "fingering mode", where dunes elongate in the approximate longitudinal direction of the resultant sand flux at their crest [35]. Both of these modes of sand transport are being recognized on Mars, from morphology [36] and dynamic motion [8]. DTR motion can also progress longitudinally downwind, rather than transversely [37, 38], which has critical implications for the numerous prior studies that had assumed the latter when interpreting wind directions and sand fluxes from bedform morphology.

Acknowledgments: This research effort for M.C. was supported in part by NASA MDAP Grant NNNH14ZDA001N.

References: [1] Bridges N. et al. (2014) *Mars 9*, Abs. #1297. [2] Banks M. et al. (2015) *Plan. Dunes Work. IV*, Abs. #8036. [3] Banks M. et al. (2018) *JGR Planets*. [4] Bridges N. et al. (2012) *Nature*. [5] Ayoub F. et al. (2014) *Nat Comm.* [6] Chojnacki M. et al. (2015) *Icarus*. [7] Chojnacki M. et al. (2018) *JGR Planets*. [8] Chojnacki M. et al. (2019) *Geology*. [9] Runyon K. et al. (2017) *Earth Plan. Sci. Lett.* [10] Sullivan R. (2008) *JGR Planets*. [11] Sullivan & Kok (2017) *JGR Planets*. [12] Bridges N. et al. (2017) *JGR Planets*. [13] Ewing R. et al. (2017) *JGR Planets*. [14] Lapotre et al. (2016) *Science*. [15] Diniega S. et al (2017) *Geol. Soc. Lond.* [16] Ewing R. et al. (2010) *JGR Planets*. [17] Fenton and Hayward (2010) *Geomorphology*. [18] Farley et al. (2014) *Science*. [19] Kite E. et al. (2013) *Geology*. [20] Chojnacki M. et al. (2017) *Aeol. Res.* [21] Roback K. et al. (2019) *LPSC*, Abs. #3169. [22] Chojnacki et al. (2019) *AGU*, Abs. #P433861. [23] Silvestro S. et al. (2010) *Geophys Res Lett.* [24] Chojnacki M. et al. (2016) *JGR Planets*. [25] Golombek M. et al. (2010) *JGR Planets*. [26] Fenton L. et al. (2018) *JGR Planets*. [27] Chojnacki et al. (2019) *GSA*, Abs. #317967. [28] Silvestro S. et al. (2019) *LPSC*, Abs. #1800. [29] Bourke M. et al. (2003) *LPSC*, Abs. #2090. [30] Geissler P. and J. Wilgus (2017) *Aeol. Res.* [31] Berman D. (2018) *Icarus*. [32] Kok (2012) *Phys. Rev. Lett.* [33] Siminovich et al. (2019) *JGR*. [34] Rubin D. and R. Hunter (1987) *Science*. [35] Courrech du Pont S. et al. (2014) *Geology*. [36] Fernandez-Cascales L. (2018) *Earth Planet. Sci. Lett.* [37] Vaz D. et al. (2017) *Aeol. Res.* [38] Silvestro S. et al. (2016) *GRL*.